The Effect of Bacterial Growth Phase and Culture Concentration on U(VI) Removal from Aqueous Solution

Janice P. L. Kenney[1], Tim Ellis[2], Felix S. Nicol[1], Alexandra Porter[2], and Dominik J. Weiss[1]

1-Department of Earth Science and Engineering, Imperial College London, London, United Kingdom

2-Department of Materials, Imperial College London, London, United Kingdom

Abstract

Bacteria play a key role in controlling the mobility of contaminants, such as uranium (U), in the environment. Uranium could be sourced from disposed radioactive waste, derived either from surface disposal trenches for Low Level Waste (LLW) that, because of the waste type and disposal concept, would typically present acidic conditions (both aerobic and anaerobic), or from the geological disposal of LLW or Intermediate Level Waste (ILW) that, because of the waste type and the disposal concept, would typically present alkaline conditions (anaerobic only). In disposed radioactive waste, there could be variable amounts of cellulosic material. Bacterial cells may be living in a range of different growth phases, depending on the growth conditions and nutrients available at the time any waste-derived U migrated to the cells. A key knowledge gap to date has been the lack of a mechanistic understanding of how bacterial growth phases (exponential, stationary, and death phase) affect the ability of bacteria to remove U(VI) from solution. To address this, we first characterised the cells using potentiometric titrations to detect any differences in proton binding to proton active sites on *Pseudomonas putida* cells at each growth phase under aerobic conditions, or under anaerobic conditions favourable to U(IV) reoxidation. We then conducted batch U(VI) removal experiments with bacteria at each phase suspended in 1 and 10 ppm U aqueous solutions with the pH adjusted from 2-12 as well as with culture concentrations from 0.01 - 10 g/L, to

identify the minimal concentration of bacteria in solution necessary to affect U removal. We found that, in death phase, *P. putida* cells exhibited double the concentration of proton active sites than bacteria grown to exponential and stationary phase. However, we did not see a difference in the extent of U(VI) removal, from a 10 ppm U solution, between the different growth phases as a function of pH (2 to 12). Culture concentration affected U removal between pH 2-8, where U removal decreased with a decreasing concentration of cells in solution. When the pH was 10-12, ≤ 55% of U precipitated abiotically. The presence of bacteria in solution (0.01 – 10 g/L), regardless of growth phase, increased the precipitation of U from ≤ 55% up to 70-90%, accumulating inside the cells and on the cell walls as ~0.2 µm uranyl phosphate precipitates. These precipitates were also found at low pH with the exception of cells at exponential growth phase. This study demonstrates that growth phase affects the proton-active site concentration but not the extent of U bound to *P. putida* cells and that growth phase dictates the form of U removed from solution. Since the pH of trench-disposed LLW is controlled by the degradation of cellulosic waste, leading to acidic conditions (pH 4-6), bacterial concentrations would be expected to highly affect the extent of U removed from solution. The cement in grouted ILW and LLW, for geologic disposal, will allow for the development of extremely high pH values in solution (pH 9-13), where even the smallest concentrations of bacteria were able to significantly increase the removal of U from solution under aerobic conditions, or under anaerobic conditions favourable to U(IV) reoxidation.

1.0 Introduction

Radionuclides can be released into the environment *via* the degradation of radioactive waste disposal containers and the evolution of their associated wasteform. The release of radionuclides, such as uranium (U), from low- and intermediate-level waste (LLW and ILW, respectively) containers will occur under different pH environments, depending on the means

and location of disposal. Historically, disposal of LLW was made to trenches at the Low Level Waste Repository (LLWR) in the UK, where the combination of the corrosion of metal containers and the degradation of cellulosic wastes has led to mildly acidic pH conditions (Cummings and Raaz, 2011). Current and future disposal of grouted LLW and plans for future geologic disposal of ILW, which will be grouted and backfilled with cement, would allow for the development of very alkaline solution (pH 9-13; Francis et al., 1997; Cummings and Raaz, 2011). LLW and ILW may be in an aerobic environment during on-site storage, the operation phase, and the early stages of post-closure, and therefore it is important to understand how U will behave under both pH regimes under aerobic conditions. Additionally, under geologic disposal conditions which contain bicarbonate, along with Fe or Mn, U(IV) may be reoxidized to U(VI) in anaerobic solutions (Wan et al., 2005). Outside the geochemically disturbed near-field zone there will be sharp geochemical gradient to the pre-existing natural conditions of the host rock, and thereby a need to understand the behaviour of radionuclides across of range of geochemical conditions.

Bacteria are ubiquitous in the environment, persisting in rock bodies beneath the earth's surface (Pedersen and Ekendahl, 1990), and would therefore be inevitably found in the near-field environment of radioactive waste disposal sites as well as within the sites as introduced via geologic disposal facility (GDF) construction, operation, and from the waste itself. Due to the variability of waste materials disposed of in LLW and ILW, the concentration of cellulosic material available to be solubilised would also be variable (Bourbon and Toulhoat, 1996). Aqueous organic matter dissolved from the waste would be a nutrient source for the bacteria, acting as a carbon source for bacterial growth and therefore bacterial growth phase may vary throughout a disposal site. Respective bacteria populations may be living in a variety of growth phases when waste-derived U migrates from the disposal wasteform and interacts with the evolving natural system, depending on the influx of carbon sources to the

system, from exponential growth, to stationary phase, to death phase, where stationary or death phase may persist in aqueous environments for long periods of time. Microorganisms undergo varying physiological processes resulting in various exudates and cell wall protein expression as a function of changing growth phase. Currently there is little information available concerning how the various growth phases may affect the ability of bacteria to adsorb or precipitate uranium across the pH ranges relevant to radioactive waste disposal.

In bacteria-free systems, U would tend to adsorb to rocks and minerals below pH 9. Above pH 9, U would tend to precipitate abiotically, as a sodium uranium mineral, in solutions rich in NaCl (e.g. Bots et al., 2014; Kenney et al., 2017), but it is unclear what role bacteria will play in such higher pH environments as could be associated with some radioactive waste disposal concepts. Previous studies have shown that bacteria undergo varying physiological processes during growth, which can result in various exudates and cell wall protein expression as a function of changing growth phases (e.g. Gad et al., 2004; Azam et al., 1999; Rolfe et al., 2012; Liu et al., 2016). Limited information is available concerning how bacterial surface properties change as a function of growth phase, and the information that is available shows that the site density of functional groups on the cell surface or associated with bound capsular extracellular polymeric substance (EPS) may be higher at exponential phase or death phase, depending on whether the cells are Gram-positive or Gram-negative. Daughney et al. (2011) performed surface complexation modelling on the cells of *Bacillus subtilis*, a Gram-positive bacterium, during exponential and stationary phase to determine the acidity constants of the sites available for binding and the concentration of those sites on the bacterial cell surface. They found that exponential phase bacteria had higher acidity constants and site concentrations than those at stationary phase. The exponential phase bacteria in that study, having more sites available for metal-binding, removed more Cd and Fe from solution than the stationary phase. Liu et al. (2016) studied the effect of growth phase on the surface

properties of *Synechococcus* cyanobacterium, a Gram-negative bacterium, and found little differences between acidity constants derived from modelling the titrations of the cells, but did find that cells in death phase had significantly higher concentrations of EPS associated with the cell surface that was produced at death phase. An increase in EPS produced during bacterial growth may lead to increased sites available for immobilising metals, such as U, however several studies have not seen a difference in the proton active sites when comparing cells with and without their EPS removed (Ueshima et al., 2008; Kenney and Fein 2011). Increased EPS may also increase the propensity for bacteria to adhere to a rock surface and thereby reduce its environmental mobility (Hong et al., 2013).

The adsorption of aqueous U(VI) onto bacterial cells has been examined in detail on bacteria in stationary growth phase and at pH values less than 9 (Fowle et al., 2000; Gorman-Lewis et al., 2005; Sheng et al., 2011; Alessi et al., 2014). Bacteria under those conditions remove nearly 100% of U at circumneutral pH values and greater than 20% removal at pH values as low as pH 1.5 (Fowle et al., 2000; Gorman-Lewis et al., 2005). Gorman-Lewis et al. (2005) also noticed that U adsorption decreased with decreasing concentration of cells in solution. At higher pH values associated with cementitious LLW and ILW disposal (pH > 9), we predict that U would precipitate abiotically, as has been seen by Kenney et al., 2017, but it is unclear whether bacteria would enhance or inhibit precipitation at those pH values.

The aim of this study was to understand how growth phase and culture concentration affect the ability of bacterial cells to remove uranium from solution. To achieve this, we first studied how growth phase affected the surface properties of the bacterium *Pseudomnas putida*, a microbe found both in soils and in the subsurface. This was done by using surface complexation modelling of potentiometric titrations to determine the acidity constants and site concentration of functional groups on the cells surface and to identify any changes as a function of growth phase. This was complemented with Fourier Transform infrared (FT-IR)

spectroscopy on the cells from different growth phases with varying pH, to identify proton active functional groups available for binding. We then conducted batch U removal experiments as a function of pH, growth phase, and culture concentration. Cells incubated with and without U were analysed using FT-IR spectroscopy to elucidate which functional groups were responsible for U removal from solution. In order to confirm if the U-bacteria complexes observed using FT-IR spectroscopy formed due to adsorption or precipitation and to identify the composition of the precipitates, transmission electron microscopy (TEM) combined with energy dispersive x-ray spectroscopy (EDX) were used to generate spatially resolved elemental maps of the mineral precipitates within the cells.

2.0 Material and Methods

2.1 Bacterial Growth

Cells of *P. putida* were cultured aerobically at 37°C in 10 mL of Luria-Bertani medium and incubated for 24 h. The biomass was transferred to 1 L of the same growth medium and incubated for enough time to bring them to the desired growth phase (exponential, stationary, and death phase). Cells were harvested at 8 h for exponential phase, 24 h for stationary phase, and 96 h for death phase. Each phase was monitored using optical density at 540 nm using a UV-vis spectrometer, with bacteria-free medium as a background to gauge growth.

After incubation, the biomass was separated from the growth media via centrifugation at 4000 rpm and washed (Kenney and Fein, 2011). Briefly, cells were rinsed 5 times with a clean 0.1 M NaCl electrolyte solution to remove all growth media from the cells so any possible growth would be retarded. After the washing procedure the cells were centrifuged twice at 4000 rpm for 30 minutes, removing as much solution as possible, in order to determine the wet mass of the bacterial pellet to be used in potentiometric titrations and U batch experiments. All further discussion of mass will refer to the wet mass of bacterial cells.

2.2 Potentiometric Titrations

Potentiometric titrations were conducted on suspensions of bacteria (30-50 g/L). The ionic strength of the suspensions was buffered using 0.1 M NaCl, and conducted under an N_2 atmosphere. The electrolyte was bubbled with N_2 for 60 minutes prior to suspension, in order to purge atmospheric CO_2. Titrations were carried out a minimum of three times with different cell suspensions, using a Metrohm 888 Titrando automated burette assembly and pH measurements were conducted with an SLS Electrode semi micro glass combination electrode filled with 0.1 M NaCl. The suspensions were first acidified to pH ~2.5 using 1.0 M HCl. Aliquots of 1.0 M NaOH were used to raise the pH of the suspensions up to approximately pH 9.5 before being lowered back down to pH 3 using 1.0 M HCl, to test the reversibility of proton binding. Each individual suspension was stirred throughout the titration with a magnetic stir bar.

2.3 Batch Uranium Removal Experiments

Batch experiments were conducted by measuring the change in aqueous U concentration that occurred upon exposure of an aqueous U solution to the washed *P. putida* cells. A parent solution containing approximately 10 ppm U in 0.1 M NaCl was prepared from a 1000 ppm U standard reference solution. A pellet of washed cells was suspended in the 10 ppm U solution to achieve a bacterial concentration of 1 g/L in each experiment. The parent suspensions were divided into 5 mL volumes in 15 mL polypropylene test tubes, and the solution pH of each suspension was adjusted to a desired starting pH, ranging from pH values of 3 to 12, using small aliquots of 0.1 to 1 M HCl or NaOH. The systems were allowed to equilibrate via end-over-end rotation at 24 rpm for 2 h to allow time for equilibration between the U and the cells. After equilibration the final pH was measured and the cells were separated from the solution via centrifugation at 4000 rpm and then the supernatant was

filtered through a 0.45 μm disposable nylon filter. The final concentration of U remaining in solution was determined using inductively coupled plasma-mass spectroscopy (ICP-MS) with matrix-matched standards. The concentration of U removed from solution by the cells was calculated by the difference between the initial and final U concentrations. The pH of the samples was measured before and after equilibration to identify possible drifts in hydrogen concentration.

2.4 Electron Microscopy

TEM (JEOL 2100 Plus) was used to establish whether U is removed *via* adsorption or precipitation, and to determine whether this mechanism changed as a function of growth phase. EDX spectroscopy was used to provide elemental information of cellular precipitates within different growth phases. The exposed cells were pelleted and fixed with 2.5% glutaraldehyde (Sigma) and stained with 1% osmium tetroxide (TAAB) for 30 minutes. Cells were serially dehydrated in a graded ethanol series (50%, 70%, 95% ethanol to ultrapure water) and 100% dried ethanol for 5 minutes each at respective stage before immersing samples in acetonitrile (Sigma) for 15 minutes. Samples were progressively infiltrated with a Quetol-based resin (TAAB) (8.75 g Quetol, 13.75 g nonenyl succinic anhydride, 2.5 g methyl acid anhydride, 0.62 g benzyl dimethylamine) for three days at 50%, 75% and 100% respectively, using acetonitrile diluent. Fresh resin was applied before placing samples under vacuum for 24 hours. Further fresh resin was applied before curing for 4 days at 60°C. Thin sections (70 nm) were cut directly into an aqueous reservoir using an ultramicrotome (RMC products) with a diamond knife set at a wedge angle of 35°. Sections were immediately collected on bare, 300 mesh copper TEM grids (Agar Scientific), dried and coated with 5 nm carbon (PECSII, Gatan). Samples were imaged and analysed in an FEI Titan 80–300 scanning/transmission electron microscope (S/TEM) operated at 80 kV, fitted with Cs

(image) corrector and SiLi EDX spectrometer (EDAX, Leicester UK). EDX maps were obtained over an area of 88.6 μm^2, using pixel sizes of 2 nm and dwell times of 16 μs per pixel. EDX data was processed using ESPRIT software (Bruker).

2.5 Fourier Transform Infrared Spectroscopy

FT-IR spectroscopy was conducted on a Nicolet 5700 Spectrometer using a diamond attenuated total reflection (ATR) accessory. Bacterial pellets with and without U at various pH values were pressed onto the ATR crystal and 128 scans were averaged for each sample following a background spectrum of 128 scans with a spectral resolution of 4 cm^{-1}. Spectra of the supernatant were recorded so that the aqueous supernatant spectra could be subtracted from that of the wet bacterial pellet to ensure the entire signal is coming from the U associated with the bacterial cells. All spectra were baseline corrected using asymmetric least squares fitting (Eilers, 2004) with parameters λ = 30,000 and p = 0.001, smoothed using a Savitzky–Golay filter (Savitzky and Golay, 1964) and area-normalised to the amide II band at 1548 cm^{-1} (Leone et al., 2007) using a previously developed script (Felten et al., 2015).

3.0 Results and Discussion

3.1 Characterisation of bacterial cells at various growth phases

Potentiometric titrations were conducted in triplicate and a representative titration curve is shown in Figure 1. The titrations are plotted as acid and base added during the titration:

$$(C_a - C_b)/m \quad (1)$$

where C_a and C_b are the total concentrations of acid and base (mol/L) added at each step of the titration and m is the mass (g) of bacterial cells in suspension. The bacteria at all growth phases studied exhibit significant and continuous proton buffering over the entire pH range considered (Figure 1).

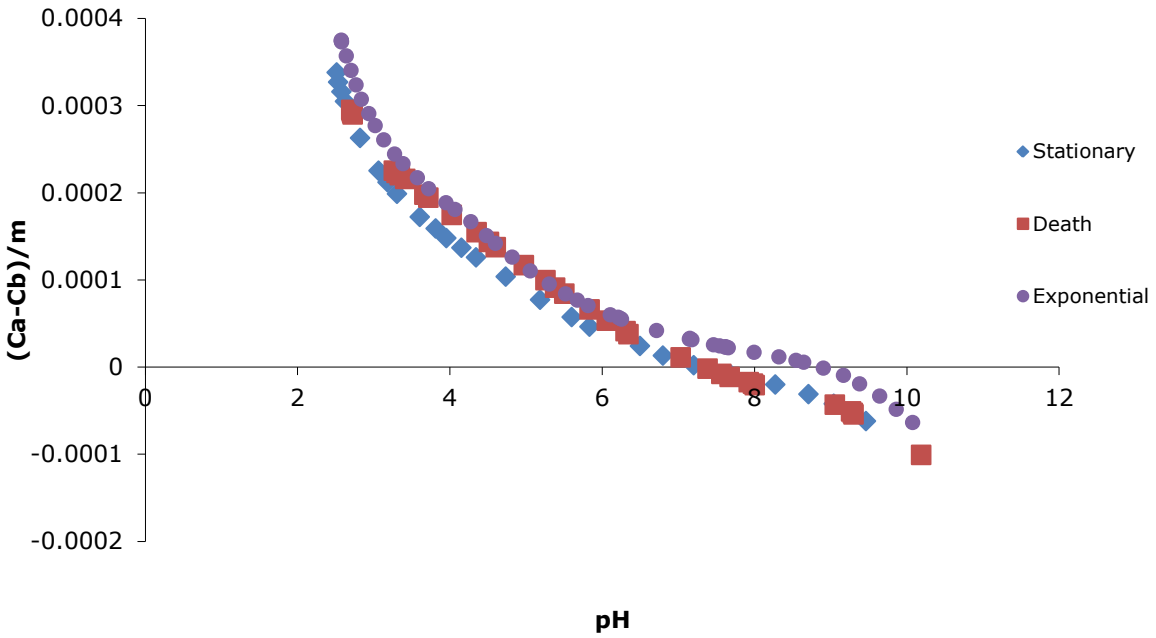

Figure 1: Potentiometric titration data for *P. putida* (30–50 g/L wet mass) biomass at Stationary (◊), Death (□), and exponential phases (○) in 0.1 M NaCl electrolyte solution. Each curve depicts a representative titration curve generated from triplicate titrations.

Titration data for each titration for the three growth phases studied here were modelled using a discrete proton-active site surface complexation model, following the approach of Fein et al. (2005). The functional groups on bacterial cell walls are represented by distinct sites that deprotonate according to the following reaction:

$$R\text{–}Site_XH^\circ \leftrightarrow R\text{–}Site_X^- + H^+ \quad (2)$$

where R represents the bacterial cell wall macromolecules to which each type of functional group, $Site_X$, is attached. The equilibrium constant (K_a) for this reaction is expressed as:

$$K_a = [R\text{–}Site_X^-]*[H^+]/ [R\text{–}Site_XH^\circ] \quad (3)$$

where [R–$Site_X^-$] and [R–$Site_XH°$] represent the concentrations of the deprotonated and protonated form of site type $Site_X$, respectively, and [H^+] represents the concentration of protons in solution. Experimental data for proton sorption to the bacterial cells were modelled with a non-electrostatic surface complexation model. This model has been used to describe the proton active sites of bacterial cells (Yee and Fein, 2001; Borrok and Fein, 2005; Johnson et al., 2007; Ueshima et al., 2008).

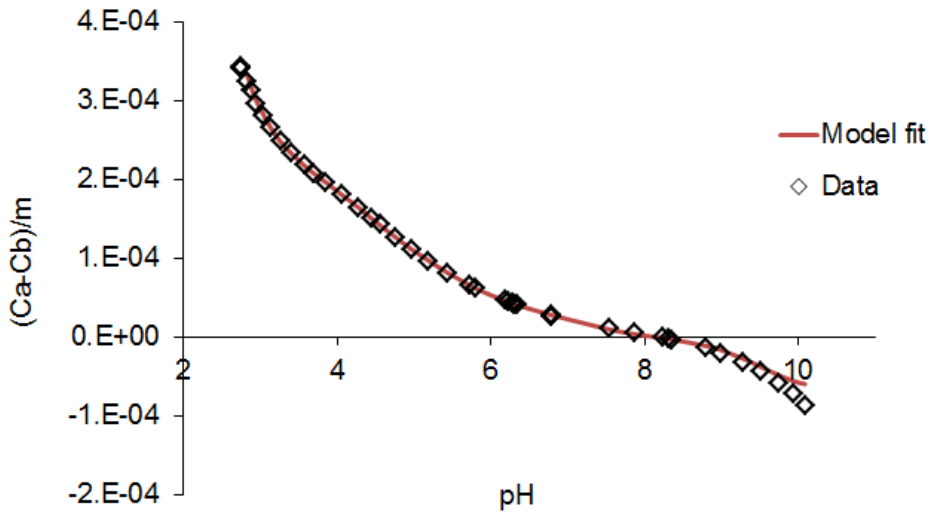

Figure 2: A representative example of the goodness of fit of the non-electrostatic model (red curve) to the potentiometric titration data (open diamonds) for *P. putida* cells at exponential phase.

We determined the total number of discrete sites necessary to account for the observed buffering capacity using FITEQL 2.0 (Westall, 1982). This was done by sequentially testing models with 1 through 5 proton-active site types until the best fit to the data was determined, with the goodness of fit for each model being quantified using the residual function in FITEQL 2.0, V(Y), where the ideal value of 1 characterizes the ideal fit of the model to the data (Westall, 1982). For each titration modelled here, a four-site model provides the best fit to the data. The 4-site models consistently yield the V(Y) values closest to 1 (average V(Y)

of 2.24), as well as the best visual fits to the data for each titration. A representative model fit to the data is presented in Figure 2.

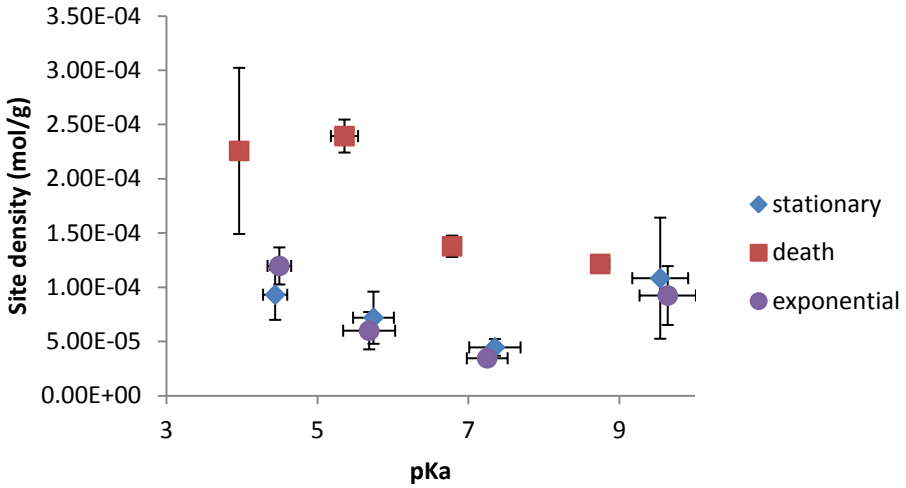

Figure 3: pKa values and their corresponding site concentrations for *P. putida* cells at exponential, stationary, and death phases. Error bars represent ±1 standard deviation from a minimum of three titrations.

The resulting calculated site concentrations and acidity constants are compiled in Figure 3. We find that the pKa values for each of the growth phases in our study were similar, only death phase cells having pKa values lying slightly lower than exponential and stationary phase. Death phase cells had at least 1σ higher site concentrations for the first three sites, with 3σ higher for the second site, and 2σ higher for the third site than the exponential and stationary cells. The pKa values and site concentration from our experiments were all within 2σ of those seen by others for a wide range of bacteria (Johnson et al., 2007; Kenney and Fein, 2011) with the exception of the concentration of proton active sites for the death phase cells in our study were higher than those of the other studies. This trend of higher site densities in death phase from *P. putida*, a Gram-negative species, is the opposite as was seen

in Daughney et al. (2001) for the Gram-positive *Bacillus subtilis*, but similar to what was seen for other Gram-negative species (Liu et al. 2016). This may be due to the fact that Gram-positive and Gram-negative cells exude EPS differently (Green and Mecsas, 2016), and therefore in our study the excess of sites in death phase could relate to an increase in cell-bound EPS. *Pseudomonas* cells have been shown to produce increased amounts of the polysaccharide alginate with decreasing carbon source and increasing growth (Conti et al., 1994) and therefore this is likely to be the polysaccharide responsible for the excess site concentration in death phase cells.

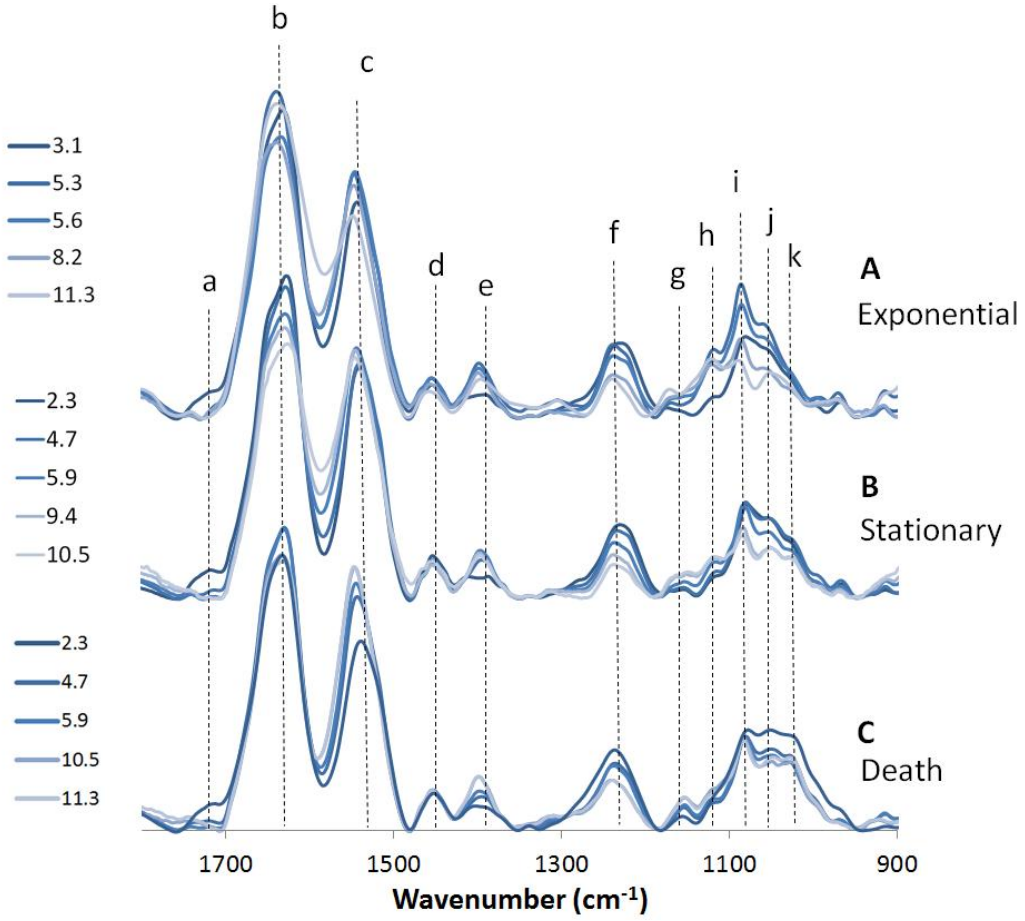

Figure 4: Area normalized FT-IR spectra of *P. putida* cells as a function of pH (dark blue to light blue shows transition from pH 2.3 to 11.3) for A) exponential, B) stationary, and C) death phase cells.

FT-IR spectroscopy was conducted on bacterial samples as a function of pH from 2.3-11.3 to determine how the functional groups of the cells change and to establish whether an increase in EPS was responsible for the increase in proton active sites in bacteria at death phase. While FT-IR spectroscopy measures all bonds in the bacterial cells, the active functional groups are those bands that change with changing pH. The FT-IR spectra of cells at exponential, stationary, and death phase is shown in figure 4 and the chemical assignment of each band is given in Table 1. Exponential, stationary, and death phase all exhibited distinct peaks that correspond to carboxyl, phosphoryl, amine, and hydroxyl groups (Table 1). These peaks will change as a function of pH if the protonation of functional groups on the cell surface change. The peaks at 1726 and 1400 cm^{-1} (peaks a and e) are directly related to the protonation and deprotonation of carboxyl groups on the bacterial cell wall, with 1726 cm^{-1} decreasing as 1400 cm^{-1} increases following the deprotonation of the carboxyl group with increasing pH. This has been observed in other studies (e.g. Jiang et al., 2004; Ojeda et al., 2008). We observe changes in the amide I band at 1637 cm^{-1}, these changes may be related to various amounts of residual water in the cells or may be related to hydroxyl groups (Table 1). Changes in the band at 1554 cm^{-1} relate to changes in amino functional groups as well as N-H and C-N bonds in amide II in proteins. Due to the overlapping nature of the peaks for phosphate groups with methyl and carboxyl bonds and with phosphates and amines that are not proton active (ie not protonating and deprotonating on the cell surface), it is difficult to assign proton-active phosphate groups to specific bands. However, deprotonation of phosphate groups can be seen via changes in peaks at 1247, 1228, 1118, 1090, 1066, and 1047 cm^{-1}.

Table 1. Assignments of important vibrational bands, compiled after Jiang et al., 2004; Parikh and Chorover, 2006, Ojeda et al., 2008

IR band	Wavenumber (cm^{-1})	Assignment
a	1726	ν_sC=O of protonated carboxylic acid groups

b	1648	stretching of C=O in amide I, associated with proteins and δO-H of water
c	1554	N-H bending and C-N stretching in amide II, associated with proteins
d	1465	δ_{as} CH_3 and δ_{as} CH_2 of lipids or proteins
e	1400	$\nu_s COO^-$ from carboxyl groups
f	1247/1228	ν_{as} P=O of phosphodiester/phosphate monoester phosphate/ ν_sC-O of COO- groups
g	1178	νC-O from carbohydrates
h	1118	ν_sC-C, ν_sP-O-C, ν_{as}C-O-C from phosphate/phosphodiesters and carbohydrates
i	1090	$\nu_s PO_2^-$ and ν_sP-O-C of the phosphodiesters
j	1066	Mixed vibrational modes of carbohydrates and phospholipids; $\nu_s PO_2^-$, δC-O-P, ν_sC-OH, C-O-C, and
k	1047	δ(P-O-P), νOH, δC-O

ν_s = symmetric stretching; ν_{as} = asymmetric stretching; δ = bending

302

303 The biggest difference between the cells at each growth phase is in the death phase cells,
304 where unlike the exponential and stationary phase cells, there is little change in spectral
305 bands above pH 4 (Figure 4), specifically in the region 1100-1000 cm^{-1}. This means that the
306 most significant differences between the phases relates to death phase having significantly
307 more proton-active carboxyl groups than the other growth phases. This supports the
308 interpretation that the increase in site concentrations observed in the surface complexation
309 modelling, was due to an increase in carboxyl groups. Alginate is a class of EPS made up of
310 D-mannuronic and L-guluronic acid assembled into β-1,4-linked blocks (Sutherland, 2001),
311 and is rich in carboxyl groups. An increase in capsular EPS around the cells would explain
312 the lack of change in the spectral data in death phase above pH 4 as this would increase peaks
313 related to carboxyl groups relative to those of phosphate (increase in 1066 and 1047 cm^{-1}
314 relative to 1090 cm^{-1}). This is further supported by the increase seen in peaks at 1066 and
315 1047 cm^{-1} as cells age from exponential to death phase, relating to an increase in EPS (Quiles
316 et al., 2010). This significant increase in carboxyl groups would drown out the differences in
317 peaks at 1066 and 1047 cm^{-1} seen in exponential and stationary phase that would relate to

deprotonation of phosphate moieties. Therefore, given the results from the cell surface characterisation, we would expect cells at death phase to be able to remove significantly more U from solution via the increased concentrations of EPS surrounding the cells, and thereby proton active groups available for U binding.

3.2 How Growth Phase and Culture Concentration Affects Uranium Removal

Uranium batch removal experiments were conducted as a function of pH for each of the bacterial growth phases studied at 10 g/L and 1 g/L concentrations of bacteria in solution (Figure 5 A and B, respectively). Each growth phase removed a similar percentage of U from solution at a given pH. Lowering the concentration of cells in solution reduced the extent of U removal from solution at pH values less than 5 and greater than 11. To test how much bacteria in solution were needed for U removal, further experiments were conducted as a function of bacterial concentration. There was no difference observed with respect to the extent of U removed from solution as a function of growth phase, which was unexpected since death phase cells had higher concentration of sites available for binding U.

Regardless of the differences in site density, U removal from solution did not change significantly as a function of bacterial growth phase. This is different to what was seen by Daughney et al. (2001), where their cells at exponential phase had significantly more sites for binding than cells at stationary phase which led to increases in the extent of Cd and Fe removed from solution from pH 2-8. However, this is similar to what was seen previously for *P. putida* by Kenney and Fein (2011), where the presence or absence of EPS did not change the extent of Cd binding to the cell walls as a function of pH.

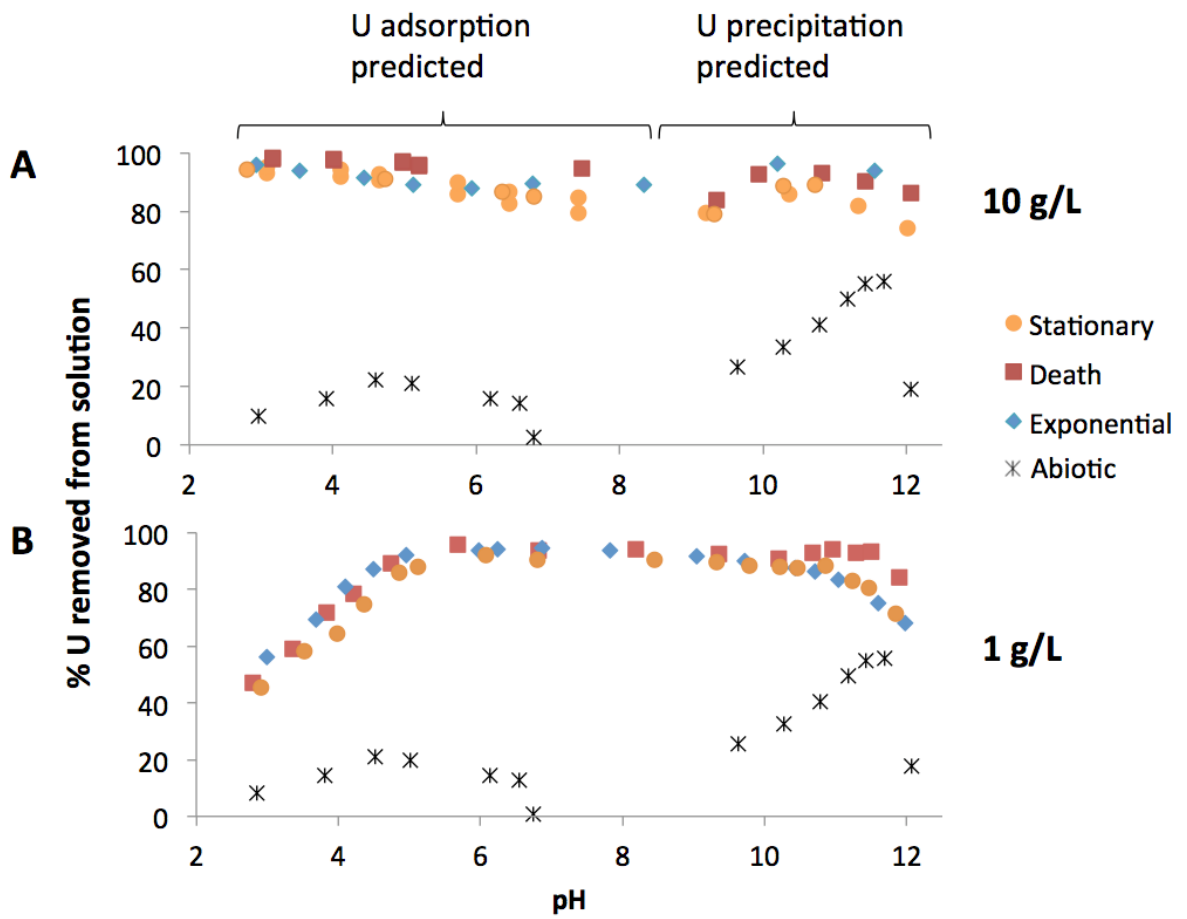

341
342

343 **Figure 5: Percentage of U removal by bacteria across all growth phases as a function of**
344 **pH in 0.1M NaCl electrolyte solution using A) 10 g/L and B) 1 g/L wet mass of bacteria**
345 **in solution. Error associated with analytical measurements is ± 5 %.**

346 Figure 6 shows the results from the batch U removal experiments as a function of pH,
347 bacterial culture concentration (0-10 g/L) and U concentration (10 and 1 ppm, Figure 6A and
348 B, respectively). The bacterial concentration experiments were conducted at stationary
349 growth phase since few changes were seen as a function of growth phase (Figure 5, see
350 discussion above). Lowering the concentration of cells in solution lowered the extent of U
351 removal from solution significantly at pH values lower than 8, but only slightly at pH values
352 greater than 8. Similar trends are seen in experiments with both U starting concentrations,
353 with decreasing U removal with decreasing concentration of cells in solution. However, the

extent of U removed from solution decreased significantly at lower pH values (< pH 8). Above pH 8 even the smallest concentrations of cells in solution were able to remove a significant concentration of U from solution when compared to abiotic removal. Therefore it is likely that U is adsorbed at lower pH values and precipitated at higher pH values, as was seen in abiotic mineral adsorption experiments with similar U concentrations and groundwater chemistry as seen by Kenney et al., (2017). This means that at pH values associated with trench disposal of LLW, there needs to be a significant amount of bacteria present to impact the mobility of U in solution. At the high pH values associated with cementitious disposal of LLW or ILW in a geological repository, only a small fraction of bacteria is needed to significantly increase the precipitation of U from solution.

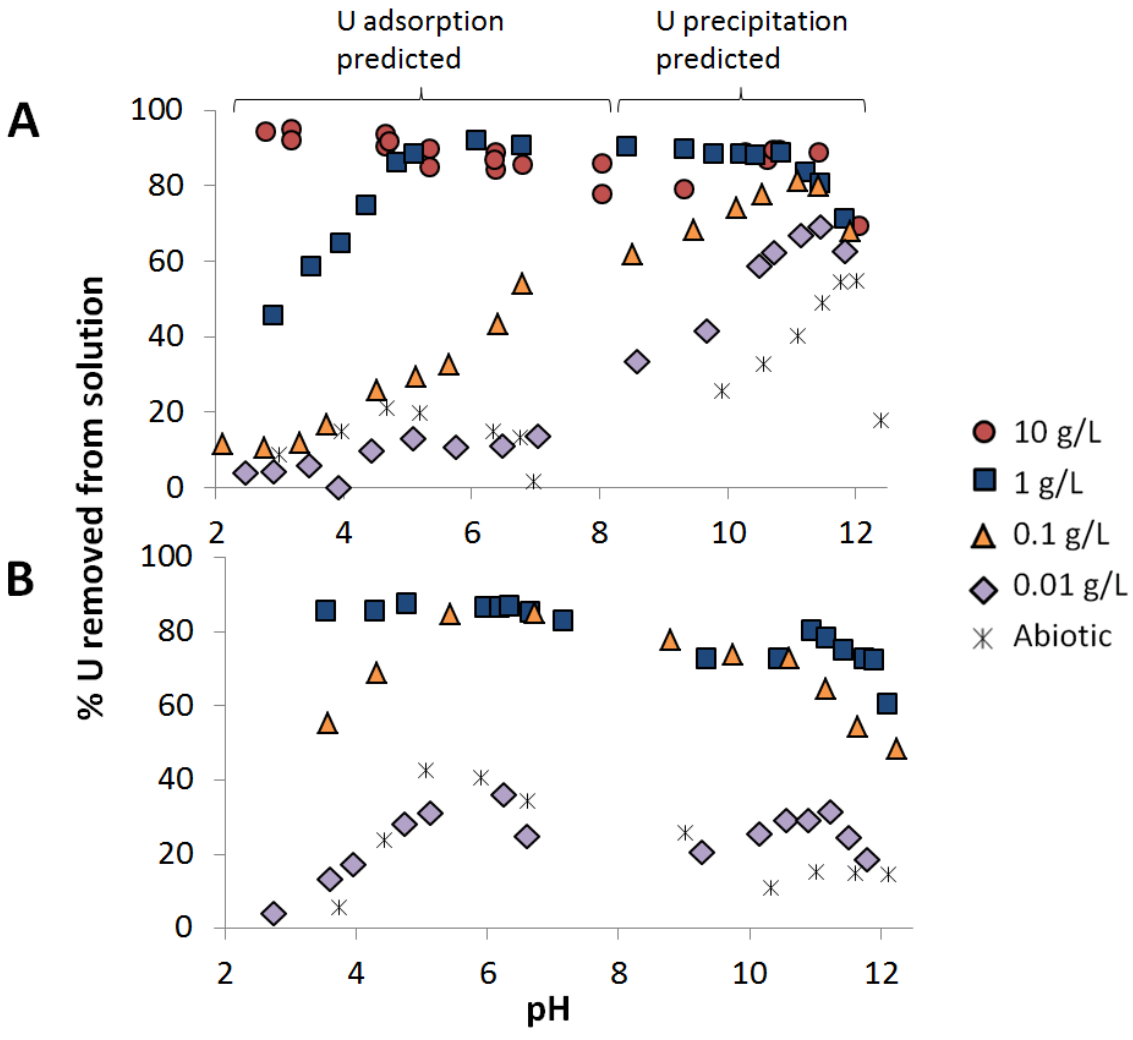

Figure 6: Percentage of U removal by bacteria at stationary phase only, as a function of U:bacteria ratios and pH in 0.1M NaCl electrolyte solution with initial U concentrations of A) 10 ppm and B) 1 ppm.

3.3 Mechanisms of Uranium Removal

The mechanism of U removal from solution as a function of growth phase was examined for cells with and without U using FT-IR spectroscopy (Figure 7), probing cells with and without U at pH 5 and pH 11 as a function of growth phase. Unlike what was observed in the batch U removal experiments, FT-IR spectroscopy (Figure 7) showed differences between the growth phases. Exponential phase cells at pH 5 showed an increase in peaks at 1240 cm^{-1} and the peak at 1228 cm^{-1} was shifted down to 1222 cm^{-1}, indicating adsorption of U to either the phosphate or carboxyl group, as well as an shift in the peak at 1074 cm^{-1} increasing in intensity and shifting to 1064 cm^{-1}, which represents mixed vibrational modes of carbohydrates and phosphodiesters. This trend was not seen in the regions where only carboxyl groups were present, therefore we attribute this shift to adsorption to the phosphate functional group. At pH 11 there is no shift in the spectra at 1240 cm^{-1} or 1066 cm^{-1} after the addition of U, but an increase in those bands. This indicates that instead of adsorption, we have the precipitation of a U-phosphate mineral. Stationary phase exhibited no shifts in their spectra at 1240 cm^{-1} at pH 5 after U was reacted with the bacteria. There is an increase in intensity in the peaks at 1066 and 1047 cm^{-1} likely associated with the precipitation of U phosphates or carbonates, and this trend was also observed but to a lesser degree at pH 11. Death phase spectra were similar to those at stationary phase, with no spectral shifts and increases in bands at 1066 and 1047 cm^{-1} for cells at pH 5 and 11.

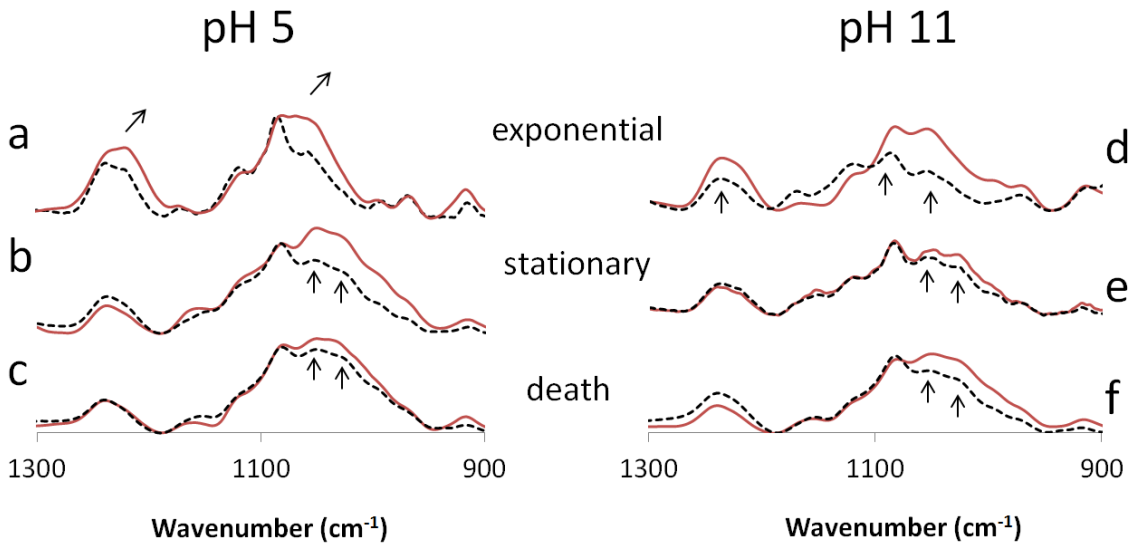

Figure 7: FT-IR spectra of bacteria at each growth phase at pH 5 (a, exponential; b, stationary; and c, death phase) and 11 (d, exponential; e, stationary; and f, death phase) with (red lines) and without (black lines) U equilibrated for 2h with 1g/L bacteria and 10ppm U in suspension.

Precipitation of U-phosphate minerals have been seen in experiments conducted at lower pH values (pH < 6) and precipitated in the cell wall or in the cytoplasm, depending on Gram type (Beveridge et al., 1983; Merroun et al., 2011; Theodorakopoulous et al., 2015). Uranium phosphate minerals were also seen to precipitate anaerobically by Alessi et al (2014), who observed the formation of a reduced, non-crystalline uranium phosphate phase associated with biomass that showed similar increases in spectral bands between 1200-900 cm^{-1}. Therefore we would expect an uranyl phosphate precipitate to be found associated with the cells and not a carbonate species. These experiments also show that cells at pH 11 are similar in spectral changes as a function growth phase when exposed to U, however at pH 5 growth phase may play a significant role in determining the mechanism of U removal. This will be further analysed with TEM below.

406

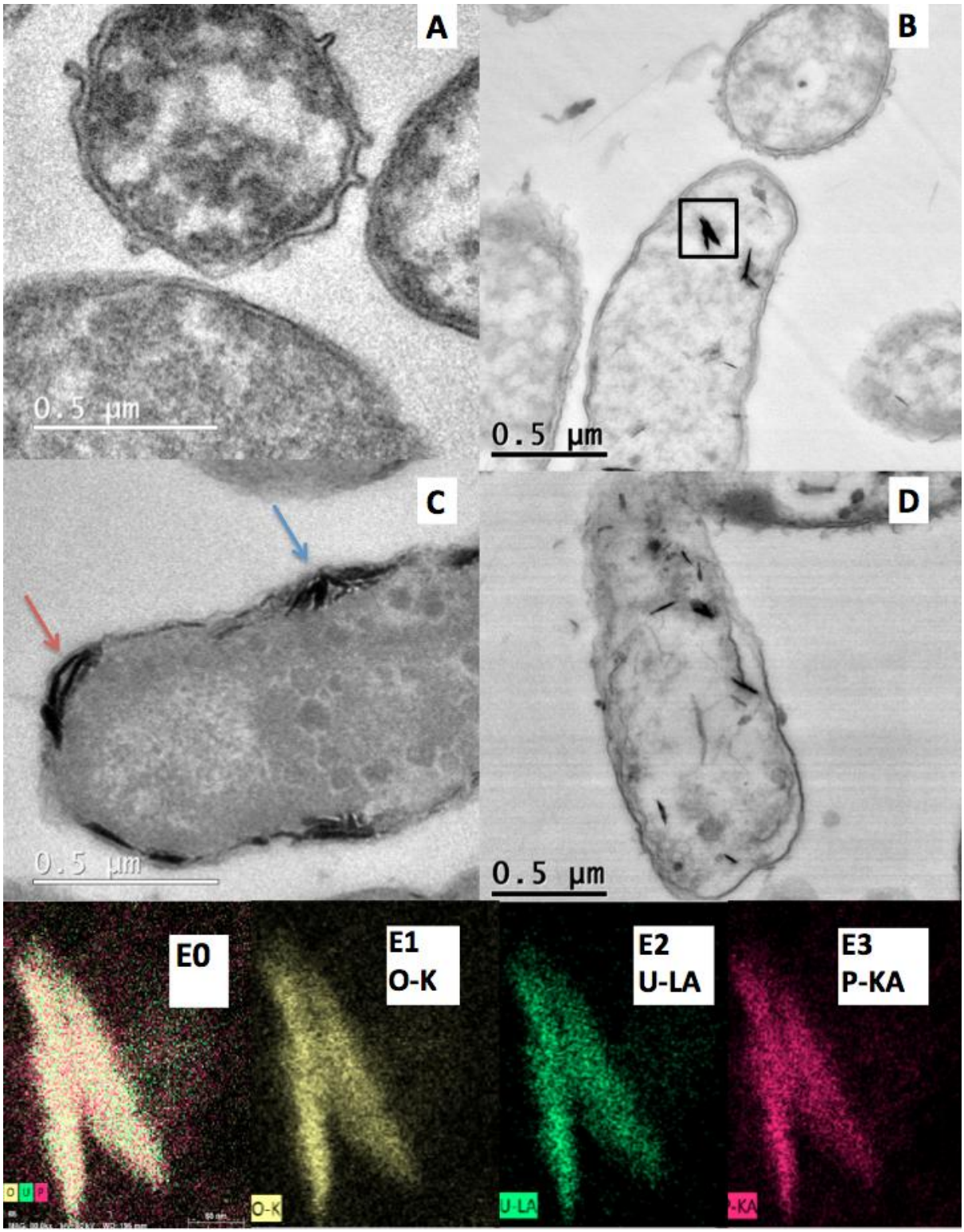

407

408 **Figure 8: TEM micrographs of *P. putida* cells at exponential phase at pH 5 (A) and pH**
409 **11 (B) and stationary phase at pH 5 (C) and pH 11 (D) with 10 ppm U. E1-E3 show**
410 **corresponding EDX elemental maps of the boxed region in B, showing the distribution**

of O, U and P in the precipitates. E0 is the overlay (O-K, U-LA, and P-KA, combined) elemental map.

To confirm whether the differences observed in the FT-IR spectra of bacterially associated U were due to adsorption or precipitation, samples from exponential and stationary phase at pH 5 and 11 were analysed using TEM (pH 5; Figure 8 A and C) and STEM (pH 11; Figure 8 B and D), and an elemental map of a typical mineral precipitate at pH 11 was analysed using STEM-EDX (Figure 8 box in B with maps E0-E3). Death phase cells were not examined since the FT-IR results show little difference between spectra of cells at stationary and death phase.

TEM data confirmed that there was a significant difference in the mechanism of U removal from solution with cells various growth phase and pH conditions. In the exponential phase at pH 5 (Figure 8A), there was no evidence of mineral precipitation within the cells. A precipitate was found in all other cells, with a length of 0.17 ± 0.6 μm long, based on 60 measurements. The cells in the exponential phase at pH 11 (Figure 8C) contained high aspect ratio needle-like precipitates within the cells. EDX elemental mapping of the chevron-shaped cluster of precipitates in Figure 8B (boxed region) are shown in Figures 8 E0-E3 and an example of the spectra are shown in Figure 9, confirming that the precipitates are rich in uranium, phosphorous and oxygen and are most probably a U-phosphate mineral. Precipitates with a similar morphology were also seen inside the cells in the stationary phase at both pH 5 and 11 (Figure 8 C and D, respectively) but the distribution of the precipitates was markedly different. Point EDX analysis of precipitates show U/P ratios of between 0.6 and 2.4, which is likely to be related to the variable P concentrations found in the cell, as the concentration of P will differ between the cytoplasm, ribosomes, nucleoid, and cell wall (Madigan and Martinko, 2006)

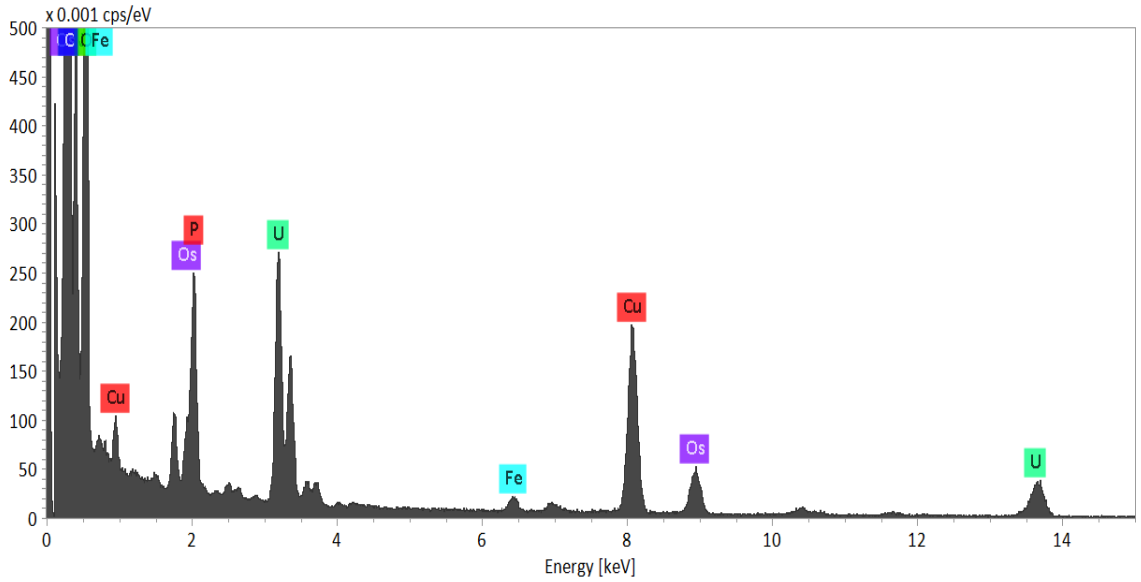

Figure 9: Example of EDX spectra from boxed region in Figure 8.

Clusters and individual precipitates were aligned with their long axis parallel to, and just inside the cell wall of the cells in the stationary phase at pH 5 (red arrow, Figure 8C) with a population of precipitates oriented with a higher contact angle to the cell wall (blue arrow, Figure 8C). In contrast, in the precipitates associated with cells at exponential and stationary phase at pH 11 were distributed within the cell interior and separated from the cell wall. The cell wall of Gram-negative bacteria are rich in lipopolysaccharides and membrane proteins, which have many phosphate moieties, and would act as a nucleation point for U-phosphate minerals. Merroun et al. (Merroun et al., 2011) found that cells grown to late exponential phase were able to precipitate U from a supersaturated U solution at pH 2-4.5 both in the cell wall and within their Gram-negative cells. In our study, the observed differentiation between precipitates occurring in the cell wall and those occurring within the cell may relate to the rupturing of cells at high pH, allowing for the U to enter the cells and precipitate with the P made available via lysis. Cells at pH 5 are not lysed and therefore the U remains at the cell wall for cells at stationary phase. As cells age from exponential phase to stationary phase, the integrity of the outer membrane may break down allowing for entry of U into the periplasmic

space and precipitate using the phosphate within the double membrane. Ohnuki et al. (2005) observed H-autunite, ($HUO_2PO_4 \cdot 4H_2O$) precipitated at ruptured regions of *Saccharomyces cerevisiae* cells grown with excess P. This is similar to our observations in solutions of pH 11 cells, where the ruptured cells allow for the U to enter the cell and scavenge intracellular P, whereas at pH 5 the U only enters the double membrane of *P. putida*.

In the context of a GDF (G, post-closure, U(VI) may still be present due to the reoxidation of U(IV) in the presence of bacteria, bicarbonate, Fe, and Mn, all things that will likely be in the subsurface environment. A GDF would have a different bacterial population than the surrounding host rock since foreign bacteria would be introduced during the engineering and operational phases, however the bacteria would likely evolve their population based on the high pH of the cement-equilibrated groundwater. Therefore the bacteria directly surrounding the GDF would likely be alkaliphilic extremophile bacteria, and as pH decreases away from the GDF the pH would lower to background levels, allowing neutralophilc bacteria to flourish. Kenney and Fein (2011) found that acidophilic, alkaliphilic, and neutralophilc bacteria rely on the same functional groups to remove the same extent of protons and metal from solution across a pH range from 1.8-11.5. Therefore, since the cells in our study passively remove U from solution via precipitation nucleated at the phosphate moieties in the cell wall, or in the cytoplasm, a wide range of bacteria in the subsurface should be able to remove U(VI) from solution in the same manner as in our study. The differences in our study may arise given that our cells were neutralophiles, and would break down at high pH, which led to precipitation of uranyl phosphates within the cells. If the cells in solution at high pH were alkaliphilic bacteria, their cell walls would remain more stable and we would see the same type of cell wall-bound precipitation as in our pH 5 experiments.

Conclusions

In this study, we investigated how growth phase and culture concentration of *P. putida* affected the removal of U from solution in the pH range between 2 and 12, under aerobic conditions. To do this we first characterised how the bacterial cells changed as a function of growth phase. This was completed via the surface complexation modelling of potentiometric titration data. We found that exponential and stationary growth phase had similar acidity constants and side densities, while death phase cells exhibited higher site densities for the first three surface sites identified. This increase in site density was reflected in the FT-IR spectroscopic results, where death phase showed a higher concentration of carboxyl groups and the lack of spectral changes with pH, and was due to an increase in capsular EPS.

However the presence of EPS did not affect the extent of U removed from solution; the same extent of U was removed from solution at any given pH value between 2-12 regardless of growth phase. Lowering the culture concentration of *P. putida* in solution did have a strong effect on the amount of U removed from solution, with decreasing U removed from solution with decreasing cells in suspension at pH values less than 8. Above 8 there was only a slight decrease in the extent of U removed from solution since even the smallest concentrations of cells in solution studied was able to precipitate significantly more U than the abiotic system. FT-IR spectroscopy coupled with TEM/STEM-EDS showed that the mechanism of U removal from solution was highly affected by pH and growth phase. During the exponential phase, cells adsorbed U at low pH and precipitated U intracellularly at high pH, whereas during the stationary phase, cells precipitated a U-phosphate in the cell membrane at low pH and intracellularly at high pH. Therefore, the form of U removed from solution may change drastically depending on the growth phase of the bacteria in solution.

Acknowledgements

We acknowledge the Natural Environment Research Council, Radioactive Waste Management Limited, and Environment Agency for the funding received for this project through the Radioactivity and the Environment (RATE) programme. We thank Prof. Mark Sephton for the use of his FT-IR spectrometer in the Department of Earth Science and Engineering at Imperial College London, and Dr. Simon Norris from RWM and Dr. Gavin Thomson for their insights in writing this manuscript.

References

Azam, T.A., Iwata, A., Nishimura, A., Ueda, S., Ishihama, A., 1999. Growth phase-dependent variation in protein composition of the Escherichia coli nucleoid. Journal of Bacteriology, 181(20): 6361-6370.

Barkleit, A., Moll, H., Bernhard, G., 2009. Complexation of uranium(VI) with peptidoglycan. Dalton Transactions(27): 5379-5385.

Bots, P. et al., 2014. Formation of Stable Uranium(VI) Colloidal Nanoparticles in Conditions Relevant to Radioactive Waste Disposal. Langmuir, 30(48): 14396-14405.

Bourbon, X., Toulhoat, P., 1996. Influence of organic degradation products on the solubilisation of radionuclides in intermediate and low level radioactive wastes. Radiochimica Acta, 74: 315-319.

Conti, E., Flaibani, A., Oregan, M., Sutherland, I.W., 1994. Alginate from Pseudomonas-Fluorescens and P-Putida - Production and Properties. Microbiology-Uk, 140: 1125-1132.

Daughney, C.J., Fowle, D.A., Fortin, D.E., 2001. The effect of growth phase on proton and metal adsorption by Bacillus subtilis. Geochimica Et Cosmochimica Acta, 65(7): 1025-1035.

Dunham-Cheatham, S. et al., 2011. The effects of non-metabolizing bacterial cells on the precipitation of U, Pb and Ca phosphates. Geochimica Et Cosmochimica Acta, 75(10): 2828-2847.

Felten, J. et al., 2015. Vibrational spectroscopic image analysis of biological material using multivariate curve resolution-alternating least squares (MCR-ALS). Nature Protocols, 10(2): 217-240.

Fletcher, M., 1977. Effects of Culture Concentration and Age, Time, and Temperature on Bacterial Attachment to Polystyrene. Canadian Journal of Microbiology, 23(1): 1-6.

Fowle, D.A., Fein, J.B., Martin, A.M., 2000. Experimental study of uranyl adsorption onto Bacillus subtilis. Environmental Science & Technology, 34(17): 3737-3741.

Francis, A.J. et al., 2004. Uranium association with halophilic and non-halophilic bacteria and archaea. Radiochimica Acta, 92(8): 481-488.

Gad, F., Zahra, T., Hasan, T., Hamblin, M.R., 2004. Effects of growth phase and extracellular slime on photodynamic inactivation of gram-positive pathogenic bacteria. Antimicrobial Agents and Chemotherapy, 48(6): 2173-2178.

538 Gorman-Lewis, D., Elias, P.E., Fein, J.B., 2005. Adsorption of aqueous uranyl complexes onto Bacillus
539 subtilis cells. Environmental Science & Technology, 39(13): 4906-4912.
540 Green, E.R., Mecsas, J., 2016. Bacterial Secretion Systems: An Overview. Microbiol Spectr, 4(1).
541 Heinrich, H.T.M., Bremer, P.J., McQuillan, A.J., Daughney, C.J., 2008. Modelling of the acid-base
542 properties of two thermophilic bacteria at different growth times. Geochimica Et
543 Cosmochimica Acta, 72(17): 4185-4200.
544 Janssen, M.J.F.W., Koorengevel, M.C., de Kruijff, B., de Kroon, A.I.P.M., 2000. The
545 phosphatidylcholine to phosphatidylethanolamine ratio of Saccharomyces cerevisiae varies
546 with the growth phase. Yeast, 16(7): 641-650.
547 Jiang, W. et al., 2004. Elucidation of functional groups on gram-positive and gram-negative bacterial
548 surfaces using infrared spectroscopy. Langmuir, 20(26): 11433-11442.
549 Kelly, S.D. et al., 2002. X-ray absorption fine structure determination of pH-dependent U-bacterial
550 cell wall interactions. Geochimica Et Cosmochimica Acta, 66(22): 3855-3871.
551 Kenney, J.P.L., Kirby, M.E., Cuadros, J., Weiss, D.J., 2017. A conceptual model to predict uranium
552 removal from aqueous solutions in water-rock systems associated with low-and
553 intermediate-level radioactive waste disposal. Rsc Advances, 7(13): 7876-7884.
554 Kenney, J.P.L, Fein, J.B., 2011. Cell Wall Reactivity of Acidophilic and Alkaliphilic Bacteria Determined
555 by Potentiometric Titrations and Cd Adsorption Experiments. Environ. Sci. Technol., 45,
556 4446-4452.
557 Lalonde, S.V., Smith, D.S., Owttrim, G.W., Konhauser, K.O., 2008. Acid-base properties of
558 cyanobacterial surfaces I: Influences of growth phase and nitrogen metabolism on cell
559 surface reactivity. Geochimica Et Cosmochimica Acta, 72(5): 1257-1268.
560 Leone, L. et al., 2007. Modeling the acid-base properties of bacterial surfaces: A combined
561 spectroscopic and potentiometric study of the gram-positive bacterium Bacillus subtilis.
562 Environmental Science & Technology, 41(18): 6465-6471.
563 Li, X.L. et al., 2016. Bioaccumulation characterization of uranium by a novel Streptomyces
564 sporoverrucosus dwc-3. Journal of Environmental Sciences, 41: 162-171.
565 Liang, X.J., Csetenyi, L., Gadd, G.M., 2016. Uranium bioprecipitation mediated by yeasts utilizing
566 organic phosphorus substrates. Applied Microbiology and Biotechnology, 100(11): 5141-
567 5151.
568 Liu, Y.X. et al., 2016. Cell surface acid-base properties of the cyanobacterium Synechococcus:
569 Influences of nitrogen source, growth phase and N:P ratios. Geochimica Et Cosmochimica
570 Acta, 187: 179-194.
571 Liu, Y.X. et al., 2015. Cell surface reactivity of Synechococcus sp PCC 7002: Implications for metal
572 sorption from seawater. Geochimica Et Cosmochimica Acta, 169: 30-44.
573 Maassen, C.B.M., Boersma, W.J.A., van Holten-Neelen, C., Claassen, E., Laman, J.D., 2003. Growth
574 phase of orally administered Lactobacillus strains differentially affects IgG1/IgG2a ratio for
575 soluble antigens: implications for vaccine development. Vaccine, 21(21-22): 2751-2757.
576 Madigan, M., Martinko, J. (Eds.), 2006. Brock Biology of Microorganisms, 11th ed.
577 Prentice. ISBN: 0131443291
578 Marshall, K.C., 1986. Adsorption and Adhesion Processes in Microbial-Growth at Interfaces.
579 Advances in Colloid and Interface Science, 25(1): 59-86.
580 Merroun, M.L. et al., 2011. Bio-precipitation of uranium by two bacterial isolates recovered from
581 extreme environments as estimated by potentiometric titration, TEM and X-ray absorption
582 spectroscopic analyses. Journal of Hazardous Materials, 197: 1-10.
583 Ojeda, J.J., Romero-Gonzalez, M.E., Bachmann, R.T., Edyvean, R.G.J., Banwart, S.A., 2008.
584 Characterization of the cell surface and cell wall chemistry of drinking water bacteria by
585 combining XPS, FTIR spectroscopy, modeling, and potentiometric titrations. Langmuir, 24(8):
586 4032-4040.
587 Pedersen, K., Ekendahl, S., 1990. Distribution and activity of bacteria in deep granitic groundwaters
588 of southeastern sweden. Microbial Ecology, 20(1): 37-52.

589 Quiles, F., Humbert, F., Delille, A., 2010. Analysis of changes in attenuated total reflection FTIR
590 fingerprints of Pseudomonas fluorescens from planktonic state to nascent biofilm state.
591 Spectrochimica Acta Part a-Molecular and Biomolecular Spectroscopy, 75(2): 610-616.
592 Rolfe, M.D. et al., 2012. Lag Phase Is a Distinct Growth Phase That Prepares Bacteria for Exponential
593 Growth and Involves Transient Metal Accumulation. Journal of Bacteriology, 194(3): 686-
594 701.
595 Sheng, L., Fein, J.B., 2013. Uranium adsorption by Shewanella oneidensis MR-1 as a function of
596 dissolved inorganic carbon concentration. Chemical Geology, 358: 15-22.
597 Snider, C.A., Voss, B.J., McDonald, W.H., Cover, T.L., 2016. Growth phase-dependent composition of
598 the Helicobacter pylori exoproteome. Journal of Proteomics, 130: 94-107.
599 Sutherland, I.W., 2001. Biofilm exopolysaccharides: a strong and sticky framework. Microbiology-Uk,
600 147: 3-9.
601 Wan, J., Tokunaga, T.K, Brodie, E., Wang, Z., Zheng, Z., Herman, D., Hazen, T.C., Firestone, M.K.,
602 Sutton, S.R. 2005. Reoxidation of Bioreduced Uranium under Reducing Conditions. Environ.
603 Sci. Technol., 39 (16): 6162-6169
604

605

606 **Graphical Abstract**

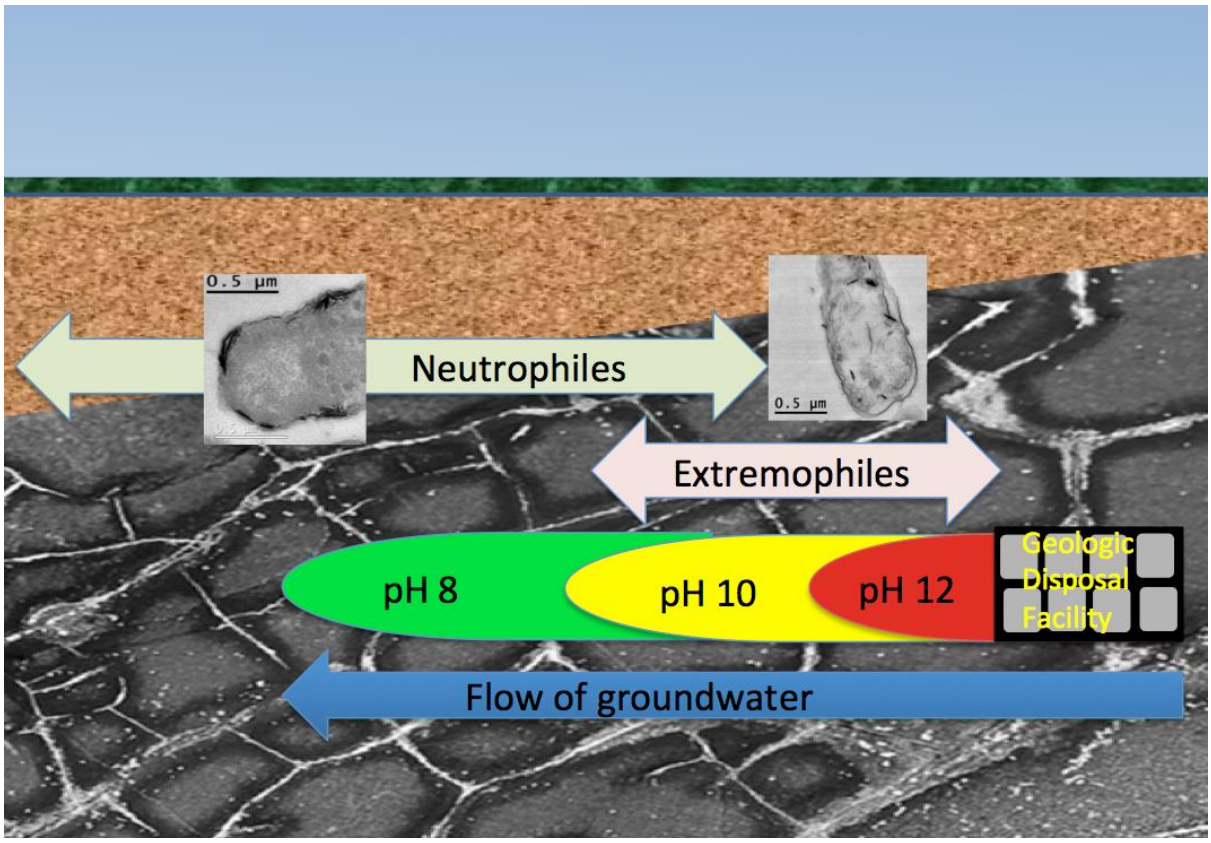

607